ACS APPLIED MATERIALS & INTERFACES
Research Article
www.acsami.org

Molecular Design and Performance of Hydroxylpyridium Sensitizers for Dye-Sensitized Solar Cells

Jianghua Zhao,[†] Xichuan Yang,*[,†] Ming Cheng,[†] Shifeng Li,[†] and Licheng Sun*[,†,‡]

[†]State Key Laboratory of Fine Chemicals, DUT−KTH Joint Education and Research Centre on Molecular Devices, Dalian University of Technology (DUT), 2 Linggong Road, 116024 Dalian, China

[‡]School of Chemical Science and Engineering, Centre of Molecular Devices, Department of Chemistry, KTH Royal Institute of Technology, Teknikringen 30, 10044 Stockholm, Sweden

Supporting Information

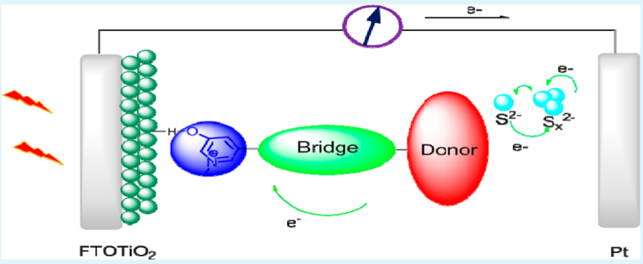

ABSTRACT: Four hydroxylpyridium organic dyes were synthesized and applied in dye-sensitized solar cells (DSSCs). Hydroxylpyridium was introduced as an electron acceptor in donor-π-conjugated bridge-acceptor (D-π-A) system. The traditional anchoring groups, such as the carboxyl group, were replaced by hydroxyl group. It was found that the existence of the hydroxylpyridium exhibits a large effect on the absorption spectra of dyes **JH401−JH404**. For **JH** series of dyes, hexylthiophene was employed as the π-conjugated bridge, and triphenylamine, phenothiazine, and their derivatives were used as the electron donor. The performances of the dyes with different structure were investigated by photophysical, photovoltaic, and electrochemical methods. When applied in the DSSCs, the sensitizer **JH401** yields the best efficiency, 2.6% (J_{sc} = 6.35 mA/cm^2, V_{oc} = 605 mV, FF = 67.6%) under 100 mW/cm^2 light illumination. Its maximum incident photon-to-current conversion efficiency (IPCE) is 80% at 440 nm light wavelength, which is the highest IPCE value achieved with hydroxyl group adsorbent organic dyes so far.

KEYWORDS: *dye-sensitized solar cells, organic dyes, anchoring group, hydroxyl adsorption, energy conversion, photovoltaic device*

INTRODUCTION

DSSCs have attracted more and more attention as an economical solar energy conversion device since O'Regan and Grätzel reported them in 1991.[1] Although metal photosensitizes, such as Ru-based complexes **N719**, **N749**, and **FT89** have yielded maximum photon-to-electron conversion efficiencies exceeding 10%,[2−4] the use of precious metals have largely restricted their development. In recent years, metal-free organic dyes have been intensively investigated due to the tailored design of the molecular structure, their high molar extinction coefficients, their environmental friendliness and low cost. Most of the organic dyes are subordinated to D-π-A structure. In this structure, the electron donor mainly affects high occupied molecular orbital (HOMO) levels of the dye. A strong electron donor, such as triphenylamine,[5−10] phenothiazine,[11] coumarin,[12−14] indoline,[15−17] and tetrahydroquinoline[18] mainly improve the HOMO levels of dye, but low unoccupied molecular orbital (LUMO) levels are only slightly altered. The π-conjugated bridge plays a major role in connecting the electron donor and the electron acceptor. Usually, a lengthened π-conjugated bridge can lead to broadened absorption spectra for the narrowed energy gap (E_g). Thiophene and its derivatives have been successfully used as a π-conjugated bridge in the molecular design of organic dyes.[19−21] When compared to electron donor and π-conjugated bridge, there are a few reports on electron acceptor and anchoring group. Cyanacrylic acid has been widely employed as an electron acceptor, such as dyes **C219**,[22] **Y123**,[23] and **TH305**.[24] Carboxyl group is utilized as an anchoring group in these kinds of organic dyes. Recently, our group has reported hydroxyl adsorbent organic dyes.[25] However, the spectra response for this kind of dyes is narrow for weak withdrawing ability of the electron acceptor. In order to obtain a widened spectral response, it is a good choice to consider pyridium as electron acceptor for its strong electron withdrawing ability.[26] As we know, there is no report on the hydroxyl adsorbent cationic organic dyes so far. So it is interesting to study the effect on the performance of the DSSCs with hydroxylpyridium serving as the electron acceptor and the anchoring group.

Herein, we report four hydroxylpyridium organic dyes (**JH401−JH404**, see Figure 1). Phenothiazine and triphenylamine derivatives were adopted as the electron donor to tune the HOMO levels of the dyes. Hexylthiophene, which can diminish the electron recombination effectively and inhibit the dye aggregation for its steric hindrance effect, was introduced as the π-conjugated bridge. Hydroxylpyridium was introduced as the electron acceptor and the anchoring group in our organic dyes. The performance of **JH** series of dyes with different

Received: March 24, 2013
Accepted: May 21, 2013
Published: May 21, 2013

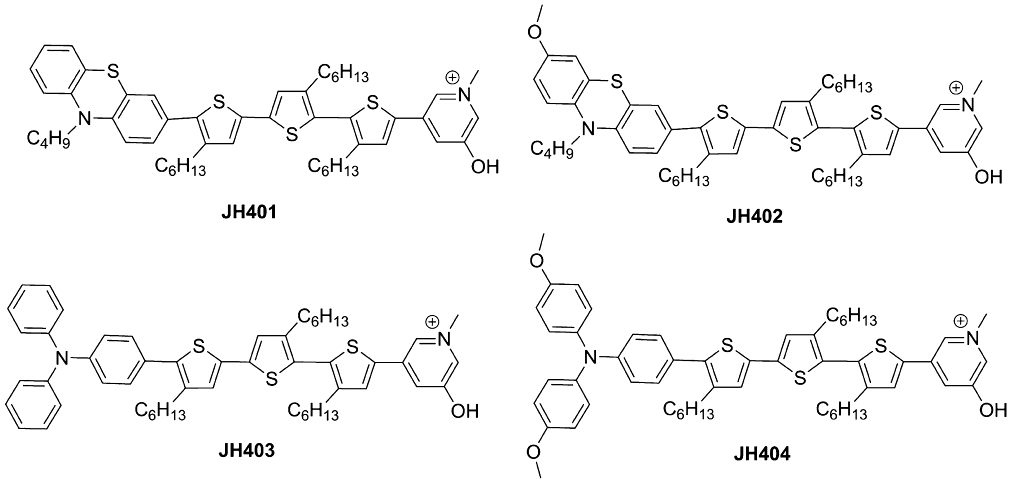

Figure 1. Structures of **JH401–JH404**.

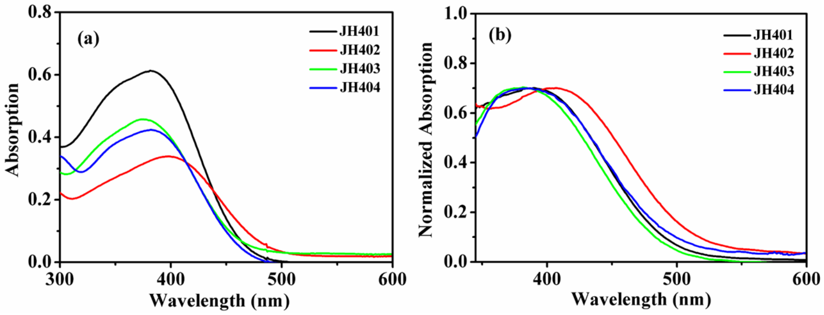

Figure 2. Absorption spectra of **JH401–JH404** (a) in solution and (b) on TiO_2 film.

structures were investigated through photophysical, photovoltaic, and electrochemical methods.

■ EXPERIMENTAL SECTION

Analytical Measurements. ^1H NMR spectra were taken with VARIAN INOVA 400 MHz (USA) using TMS as standard. MS data were obtained with GCT CA156 (UK), HP1100 LC/MSD (USA), and LC/Q-TOF MS (UK). The absorption spectra were recorded on HP8453 (USA). The absorption spectra were recorded on HP8453 (USA). Electrochemical redox potentials were obtained by cyclic voltammetry (CV) on electrochemistry workstation (BAS100B, USA). Traditional three-electrode system was used. The working electrode, auxiliary electrode, and reference electrode was a glassy carbon disk electrode, P_t-wire and Ag/Ag^+ electrode, respectively. The photocurrent–voltage (J–V) properties were measured under AM 1.5G illumination (16S–002, Solar Light Co. Ltd., USA). The incident light intensity was 100 mW/cm^2 calibrated with a standard Si solar cell. The working areas of the cells were masked to 0.159 cm^2. The J–V data were collected by an electrochemical workstation (LK9805, Lanlike Co. Ltd., China). The measurement of the IPCE was obtained by a Hypermono–light (SM–25, Jasco Co. Ltd., Japan). Electrochemical impedance spectroscopy (EIS) was measured with an impedance/gain–phase analyzer (PARSTAT 2273, USA) under dark condition, with forward bias −0.7 V. The alternate current (AC) amplitude was set at 10 mV.

Fabrication of the Dye-Sensitized Solar Cells. The DSSCs sensitized by **JH201–JH203** were fabricated by modifying the previous report.[27] A layer of 2 μm TiO_2 (13 nm paste, Heptachroma, China) was coated on the *F*-doped tin oxide conducting glass (TEC15, 15Ω/square, Pilkington, USA) by screen printing and then dried for 5 min at 120 °C. This procedure was repeated 5 times (10 μm) and finally coated by a layer (4 μm) of TiO_2 paste (DHS–SLP1, Heptachroma, China) as the scattering layer. The double-layer TiO_2 electrodes (area: 6 × 6 mm) were heated under an air flow at 500 °C for 60 min, and then cooled to room temperature. The sintered film wasfurther treated with 40 mM $TiCl_4$ aqueous solution at 70 °C for 30 min, then washed with water, and annealed at 500 °C for 60 min. After the film was cooled to room temperature, it was immersed into a 2×10^{-4} M dye bath. The electrode was then rinsed with ethanol and dried. The hermetically sealed cells were fabricated by assembling the dye-loaded film as the working electrode and Pt-coated conducting glass as the counter electrode separated with a hot–melt Surlyn 1702 film (60 μm, Dupont).

■ RESULTS AND DISCUSSION

Photophysical and Electrochemical Properties. The absorption spectra of **JH401–JH404** in CH_3COOEt and CH_3OH (2:1; v/v) solution (a) and on TiO_2 film (b) are shown in Figure 2. The characteristic data are collected in Table 1. In CH_3COOEt and CH_3OH (2:1; v/v) solution, all dyes exhibit maximal absorption wavelengths (λ_{max}) from 370 to 400 nm. It can be obviously noticed that dye **JH401** and dye **JH402** are red-shifted in comparison with dye **JH403** and dye **JH404**, respectively. The explanation for this phenomenon is probably due to a stronger electron-donating ability of the phenothiazine than that of the triphenylamine donor.[28] Obviously, the absorption spectra of all **JH** series of hydroxylpyridium dyes are shorter than previously reported cationic organic dyes.[26] It can be concluded that the introduction of the hydroxyl group as anchoring group diminishes the withdrawing ability of the electron acceptor and leads to the blue-shift of the **JH** series of dyes.

The introduction of the methoxyl group can improve the electron donating ability of the electron donor. Correspond-

Table 1. Absorption and Electrochemical Properties of the Dyes JH401–JH404

	absorption			oxidation potential		
dye	λ_{max}[a] (nm)	ε at λ_{max} (M^{-1} cm^{-1})	λ_{max}[b] on TiO_2 (nm)	E_{0-0} (V)	E_{ox} (V) (*vs.*NHE)	E_{LUMO} (V) (*vs.*NHE)
JH401	381	30400	390	2.49	0.80	− 1.69
JH402	397	17000	407	2.38	0.7	− 1.68
JH403	377	22800	382	2.53	1.14	− 1.42
JH404	383	21100	385	2.53	0.84	− 1.72

[a] Absorption spectra in solution were measured in CH_3COOEt and CH_3OH (2:1; v/v) solution (2×10^{-5} M). [b] Absorption spectra on TiO_2 film were measured with dye-loaded TiO_2 film immerged in CH_3COOEt and CH_3OH (2:1; v/v) solution.

ingly, **JH402** and **JH404** are red-shifted by 16 and 5 nm in comparison with the dye **JH401** and dye **JH403**, respectively. When anchored on TiO_2 film, the absorption spectra of **JH** series of dyes are red-shifted from 3 to 10 nm in comparison with the absorption in solution. The experiment also have proved that pyridium cannot adsorb on TiO_2 film,[26] so it is hydroxyl group adsorbent on TiO_2 film for **JH** series of dyes.

Electrochemical Properties. The electrochemical data of **JH401–JH404** are listed in Table 1. The first oxidation potential of the dyes (E_{ox}) corresponding to the HOMO energy levels of the dyes were measured by cyclic voltammetry (CV) in CH_2Cl_2 solution with 0.1 M tetrabutylammonium hexafluorophosphate ($TBAPF_6$) as supporting electrolyte, ferrocene/ferrocenium (Fc/Fc^+) as an internal reference and converted to NHE by adding 440 mV. The HOMO levels of these dyes are more positive than S/S_x^{2-} (0.65 V vs. NHE),[29] indicating that the oxidized dyes can be regenerated effectively.[30−32] Furthermore, for dyes **JH402** and **JH404**, the introduction of methoxyl group improves the HOMO levels in comparison with dyes **JH401** and **JH403**, respectively. E_{0-0} was determined by $1240/\lambda$, in which λ is from the intersection of the tangent of absorption on TiO_2 film and the X axis. E_{LUMO} was calculated by $E_{ox}-E_{0-0}$. The LUMO levels of the all dyes are sufficiently more negative than the E_{cb} (−0.5 V vs. NHE) of the TiO_2, which ensure that the excited state dyes can inject electron effectively to the E_{cb} of the TiO_2.

Molecular Orbital Calculation. To get a further insight of the geometrical configuration, electron distribution and molecular orbital of dyes **JH401–JH402**, density functional theory (DFT) calculations were performed at B3LYP/6-31+G(d) level for the geometrical optimization. The results are shown in Table 2. According to the optimized structure, we can find that the HOMO levels of all the dyes are concentrated on the electron donor, and the LUMO levels are mainly located on the electron acceptor, indicating that the effective electron separation can be obtained between the HOMO and LUMO levels. However, there is no electron density distribution on hydroxyl group in the LUMO levels.

Photovoltaic Performance of DSSCs. The photocurrent density-photovoltage (*J*–*V*) curves of DSSCs based on dyes **JH401–JH404** are shown in Figure 3. The corresponding photovoltaic data are listed in Table 3. The device sensitized by dye **JH401** exhibits the best efficiency of 2.6% with a short-current density (J_{sc}) of 6.35 mA/cm^2, an open-circuit voltage (V_{oc}) of 605 mV and a fill factor (*FF*) of 67.6%. The other solar cells sensitized by dyes **JH402**, **JH403** and **JH404** present efficiencies that range from 1.9% to 2.1%. Obviously, the J_{sc} for **JH** series of dyes do not exceed 7 mA/cm^2, which is probably due to the narrow and short absorption spectra limiting the use of long wavelengths energy. It can also be noticed that the device sensitized by **JH402** exhibits a lower V_{oc} of 519 mV in comparison with the others. The reason for this phenomenon can be explained by the CV measurement. Compared to dye **JH401** and dye **JH403**, dye **JH402** and dye **JH404** show a little

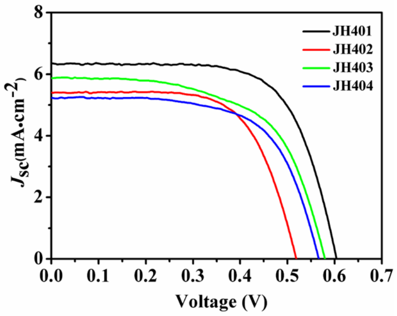

Figure 3. *J*–*V* curves of the DSSCs sensitized by dyes **JH401–JH404**.

Table 2. Optimized Structure and Electron Distribution in HOMO and LUMO Levels of the JH Series of Dyes

Dye	Optimized Structure	HOMO	LUMO
JH401	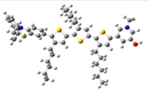	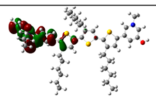	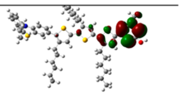
JH402	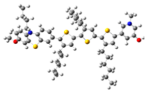	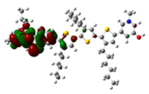	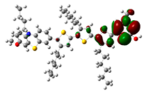
JH403	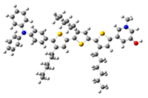	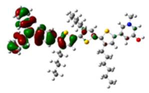	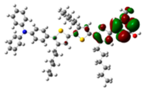
JH404	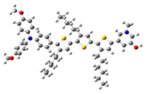	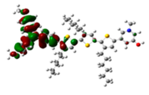	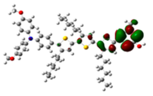

Table 3. Photovoltaic Performance[a] of DSSCs Based on the Dyes JH401−JH404

dye[b]	J_{sc} (mA/cm^2)	V_{oc} (mV)	*FF* (%)	η (%)
JH401	6.35	605	67.6	2.6
JH402	5.40	519	65.9	1.9
JH403	5.87	579	60.2	2.1
JH404	5.23	567	64.0	1.9

[a] Irradiation light: AM 1.5G simulated solar light (100 mW/cm^2) at room temperature; working area, 0.159 cm^2; electrolyte, 0.6 M DMPII, 0.1 M LiI, 0.02 M S/S$_x^{2-}$ in dry acetonitrile (AN). [b] Dye bath 2 × 10^{-4} M in MeOH/CH$_3$COOEt (1:2; v/v).

more negative HOMO levels (0.65 V vs. NHE) which are only a little positive than the redox potential of the electrolyte. Thus it is more difficult for the oxidized dyes to be regenerated by electrolyte for lack of driving force.

The photoelectron properties of the device sensitized by **JH** series of dyes were evaluated by IPCE which are shown in Figure 4. It can be noticed that the solar cells sensitized by dye **JH401** presents a maximum IPCE value of 80% at 440 nm light wavelength, which is the highest IPCE value in hydroxyl adsorbent organic dyes achieved so far. Dyes **JH402**, **JH403**, and **JH404** get a maximum IPCE value of 70% at 440 nm and 78% and 70% at 420 nm, respectively. Corresponding to absorption spectra in solution, it can be noted that the IPCE spectra for each dye become broader. Furthermore, the maximum IPCE wavelengths are red-shifted from 30 to 50 nm in comparison with the absorption on TiO$_2$ film. This is mainly because of the existence of Li$^+$ in electrolyte, which can make the absorption spectra of dyes red-shifted according to the content of the Li$^+$.

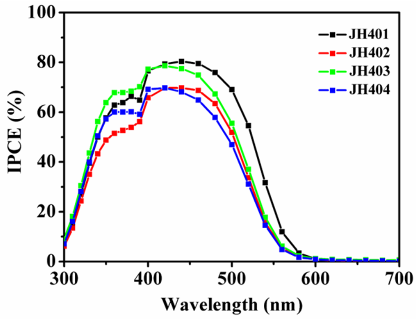

Figure 4. IPCE spectra of the DSSCs based on **JH** series of dyes.

Electrochemical Impedance Spectroscopy. Electrochemical impedance spectroscopy (EIS) analysis was employed to study interface charge transfer processes in DSSCs based on **JH401−JH404**. The measurements were scanned from 1 × 10^6 to 1 × 10^{-2} Hz. The alternate current (AC) amplitude was set at 10 mV. The Nyquist plots are displayed in Figure 5a. The larger semicircles in middle-frequency reflect the recombination resistance (R_{rec}) at TiO$_2$/electrolyte interface. Obviously, the radius of the semicircles are decreased in the order of **JH401** > **JH403** > **JH404** > **JH402**, indicating that the device sensitized by **JH401** exhibits the largest resistance between the TiO$_2$ surface and electrolyte among **JH** series of dyes. Thus under the same working condition, it is reasonable to conclude that the electron density of the E_{cb} keep the trend **JH401** > **JH403** > **JH404** > **JH402**. According to the formula: $E_f = E_c + \ln(n_c/N_c)$,[33] where E_f and E_{cb} are the Fermi energy and the conduction band edge energy, respectively, n_c is the density of conduction band electrons, and N_c is the effective density of conduction band states. As we know, the V_{oc} was determined by the potential of the redox shuttle and the E_f. We can conclude from the formula that the V_{oc} could be in accordance with the trend of **JH401** > **JH403** > **JH404** > **JH402**. The electron lifetimes could be extracted from the angular frequency (ω_{min}) at the middle-frequency peaks of the bode plots according to the formula $\tau = 1/\omega_{min}$, The electron lifetimes obtained by the bode plots are 373, 95, 251, and 184 ms, respectively, which decrease in the order of **JH401** > **JH403** > **JH404** > **JH402**. Also, we can obtain the effective diffusion length (L_n), which could be expressed for the competition between charge collection and recombination $(L_n) = L\ (R_{ct}/R_t)^{1/2}$, R_{ct} represents charge-transfer resistance at dye/TiO$_2$/electrolyte interface related to the electron recombination, R_t represents the electron transport resistance in TiO$_2$ film, and L is the thickness of TiO$_2$ film).[34] For **JH** series of dyes, the L_n are 21 μm for **JH401**, 15 μm for **JH402**, 18 μm for **JH403**, and 16 μm for **JH404**, respectively, which are all longer than the thickness of the TiO$_2$ film (14 μm), indicating that photogenerated electrons can be collected effectively.

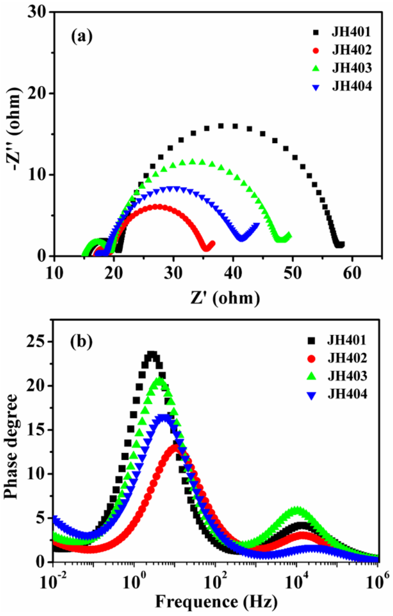

Figure 5. Nyquist plots and bode plots of DSSCs based on dyes **JH401−JH404**.

■ CONCLUSION

To study the effect of hydroxylpyridium as electron acceptor for the organic dyes on the performance of DSSCs, we designed a series of the hydroxylpyridium sensitizers (**JH401−JH404**) and investigated. The results show that different electron donating groups of the organic dyes exhibits different photophysical, photovoltaic, and electrochemistry properties. Furthermore, it is interesting to find that the existence of the hydroxyl group have largely blue-shifted the absorption of the **JH** series of the dyes for its electron donating ability. The electrochemical properties of the **JH** series of dyes ensure efficient electron injection and regeneration. DFT studies imply that the effective electron separation can be achieved in the HOMO levels and the LUMO levels. When applied in the DSSCs, the device sensitized by **JH401** yields the highest efficiency of 2.6% under the 100 mW/cm^2 light illumination, and the IPCE value are reaching 80% at 440 nm light wavelength. Furthermore, the EIS spectra provide an insight into surface recombination processes of the DSSCs sensitized by the **JH** series of the dyes. To obtain a higher efficiency, the structure modification of dye **JH401** and the related work is in progress.

ASSOCIATED CONTENT

Supporting Information

Detailed synthetic routes and characteristic of the synthesized compounds. This material is available free of charge via the Internet at http://pubs.acs.org/.

AUTHOR INFORMATION

Corresponding Author

* E-mail: yangxc@dlut.edu.cn (X.Y.); lichengs@kth.se (L.S.). Fax: +86 411 84986250 (X.Y.); +46-8-791-2333 (L.S.). Tel: +86 411 84986247.

Notes

The authors declare no competing financial interest.

ACKNOWLEDGMENTS

We gratefully acknowledge the financial support of this work from China Natural Science Foundation (Grant 21076039, Grant 21276044, Grant 21120102036 and 20923006), the National Basic Research Program of China (Grant 2009CB220009), the Swedish Energy Agency, K&A Wallenberg Foundation, and the State Key Laboratory of Fine Chemicals (KF0805), the Program for Innovative Research Team of Liaoning Province (Grant LS2010042).

REFERENCES

(1) O'Regan, B.; Grätzel, M. *Nature* **1991**, *353*, 737−740.

(2) Nazeeruddin, M. K.; Zakeeruddin, S. M.; Grätzel, M. *Inorg. Chem.* **1999**, *38*, 6298−6305.

(3) Nazeeruddin, M. K.; Pechy, P.; Grätzel, M. *J. Am. Chem. Soc.* **2001**, *123*, 1613−1624.

(4) Funaki, T.; Funakoshi, H.; Kitao, O.; Komatsuzaki, N. O.; Kasuga, K.; Sayama, K.; Sugihara, H. *Angew. Chem., Int. Ed.* **2012**, *51*, 734−7355.

(5) Hagberg, D. P.; Edvinsson, T.; Marinado, T.; Bochco, G.; Hagfeldt, A.; Sun, L. *Chem. Commun.* **2006**, *21*, 2245−2247.

(6) Tian, H.; Yang, X.; Chen, R.; Zhang, R.; Hagfeldt, A.; Sun, L. *J. Phys. Chem. C.* **2008**, *112*, 11023−11033.

(7) Xu, M.; Zhang, M.; Pastore, M.; Li, R.; Angelis, F. D.; Wang, P. *Chem. Sci.* **2012**, *3*, 976−983.

(8) Yum, H.; Hagberg, D. P.; Moon, S. J.; Karlsson, K. M.; Marinado, T.; Sun, L.; Hagfeldt, A.; Nazeeruddin, M. K.; Grätzel, M. *Angew. Chem., Int. Ed.* **2009**, *48*, 1576−1580.

(9) Kitamura, T.; Ikeda, M.; Shigaki, K.; Inoue, T.; Anderson, N. A.; Lian, T.; Yanagida, S. *Chem. Mater.* **2004**, *16*, 1806−1812.

(10) Qin, H.; Wenger, S.; Xu, M.; Gao, F.; Jing, X.; Wang, P.; Zakeeruddin, S. M.; Grätzel, M. *J. Am. Chem. Soc.* **2008**, *130*, 9202−9203.

(11) Tian, H.; Yang, X.; Chen, R.; Li, L.; Hagfeldt, A.; Sun, L. *Chem. Commun.* **2007**, *43*, 3741−3743.

(12) Hara, K.; Sayama, K.; Ohga, Y.; Shinpo, A.; Suga, S.; Arakawa, H. *Chem. Commun.* **2001**, *6*, 569−570.

(13) Wang, Z. S.; Cui, Y.; Hara, K.; Dan-Oh, Y.; Kasada, C.; Shinpo, A. *Adv. Mater.* **2007**, *19*, 1138−1141.

(14) Hara, K.; Wang, Z.; Sato, T.; Furube, A.; Katoh, R.; Sugihara, H.; Dan-oh, Y.; Kasada, C.; Shinpo, A.; Suga, S. *J. Phys. Chem. B.* **2005**, *109*, 15476−15482.

(15) Zhu, W.; Wu, Y.; Wang, S.; Li, W.; Li, X.; Chen, J.; Wang, Z. S.; Tian, H. *Adv. Funct. Mater.* **2011**, *21*, 756−763.

(16) Liu, B.; Zhu, W.; Zhang, Q.; Wu, W.; Xu, M.; Ning, Z.; Xie, Y.; Tian, H. *Chem. Commun.* **2009**, *13*, 1766−1768.

(17) Kuang, D.; Uchida, S.; Humphry-Baker, R.; Zakeeruddin, S. M.; Grätzel, M. *Angew. Chem., Int. Ed.* **2008**, *47*, 1923−1927.

(18) Chen, R.; Yang, X.; Tian, H.; Wang, X.; Hagfeldt, A.; Sun, L. *Chem. Mater.* **2007**, *19*, 4007−4015.

(19) Chen, R.; Yang, X.; Tian, H.; Sun, L. *J. Photochem. Photobiol. A: Chem.* **2007**, *189*, 295−300.

(20) Koumura, N.; Wang, Z.; Mori, S.; Miyashita, M.; Suzuki, E.; Hara, K. *J. Am. Chem. Soc.* **2008**, *130*, 4202−4203.

(21) Choi, H.; Baik, C.; Kang, S. O.; Ko, J.; Kang, M. S.; Nazeeruddin, M. K.; Grätzel, M. *Angew. Chem., Int. Ed.* **2008**, *47*, 327−330.

(22) Zeng, W.; Cao, Y.; Bai, Y.; Wang, Y.; Shi, Y.; Zhang, M.; Wang, F.; Pan, C.; Wang, P. *Chem. Mater.* **2010**, *22*, 1915−1925.

(23) Tsao, H. N.; Yi, C.; Moehl, T.; Yum, J. H.; Zakeeruddin, S. M.; Nazeeruddin, M. K.; Gratzel, M. *ChemSusChem* **2011**, *4*, 591−594.

(24) Tian, H.; Yang, X.; Cong, J.; Chen, R.; Liu, J.; Hao, Y.; Hagfeldt, A.; Sun, L. *Chem. Commun.* **2009**, *45*, 6288−6290.

(25) Li, S.; Yang, X.; Cheng, M.; Zhao, J.; Wang, Y.; Sun, L. *Tetrahedron Lett.* **2012**, *53*, 3425−3428.

(26) Cheng, M.; Yang, X.; Li, J.; Chen, C.; Zhao, J.; Wang, Y.; Sun, L. *Chem.—Eur. J.* **2012**, *18*, 16196−16202.

(27) Teng, C.; Yang, X.; Li, S.; Cheng, M.; Hagfeldt, A.; Sun, L. *J. Phys. Chem. C* **2010**, *114*, 9101−9110.

(28) Tian, H.; Yang, X.; Cong, J.; Chen, R.; Liu, J.; Hao, Y.; Sun, L. *Dyes Pigm.* **2010**, *84*, 62−68.

(29) Cong, J.; Yang, X.; Hao, Y.; Lars, K.; Sun, L. *RSC Adv.* **2012**, *2*, 3625−3629.

(30) Hagfeldt, A.; Grätzel, M. *Chem. Rev.* **1995**, *95*, 49−68.

(31) Bond, A. M.; Deacon, G. B.; Howitt, J.; MacFarlane, D. R.; Spiccia, L.; Wolfbauer, G. *J. Electrochem. Soc.* **1999**, *146*, 648−656.

(32) Kalyanasundaram, K.; Grätzel, M. *Chem. Rev.* **1998**, *177*, 347−414.

(33) Boschloo, G.; Häggman, L.; Hagfeldt, A. *J. Phys. Chem. B* **2006**, *110*, 13144−13150.

(34) Kuang, D.; Ito, S.; Wenger, B.; Klein, C.; Moser, J.; Humphry-Baker, R.; Zakeeruddin, S. M.; Grätzel, M. *J. Am. Chem. Soc.* **2006**, *128*, 4146−4154.